PCCP

ARTICLE TYPE

Cite this: DOI: 00.0000/xxxxxxxxxx

# Photofragmentation specificity of photoionized cyclic amino acids (diketopiperazines) as precursors of peptide building blocks (Electronic Supplementary Information)

Darío Barreiro-Lage,[*a] Jacopo Chiarinelli,[b] Paola Bolognesi,[*b] Robert Richter,[c] Henning Zettergren,[d] Mark H. Stockett,[d] Sergio Díaz-Tendero,[a,e,f] and Lorenzo Avaldi[b]

## 1 Electronic Supplementary Information

This ESI material contains information on:

1. The cGG and cGG ion-neutral coincidence experiments performed at three different photon energies, Figures 1 and 2.
2. Stationary points of the potential energy surface corresponding to the fragmentation channels of $cAA^+$, $cGA^+$ and $cGG^+$, Figures 3-5.
3. *Single-step* mechanisms leading to tautomerization of the three oxazolidinone derivatives discussed in main text, Figure 6.
4. Statistics of the ADMP molecular dynamics simulations for $cAA^+$, $cGA^+$ and $cGG^+$, Tables 1-3.

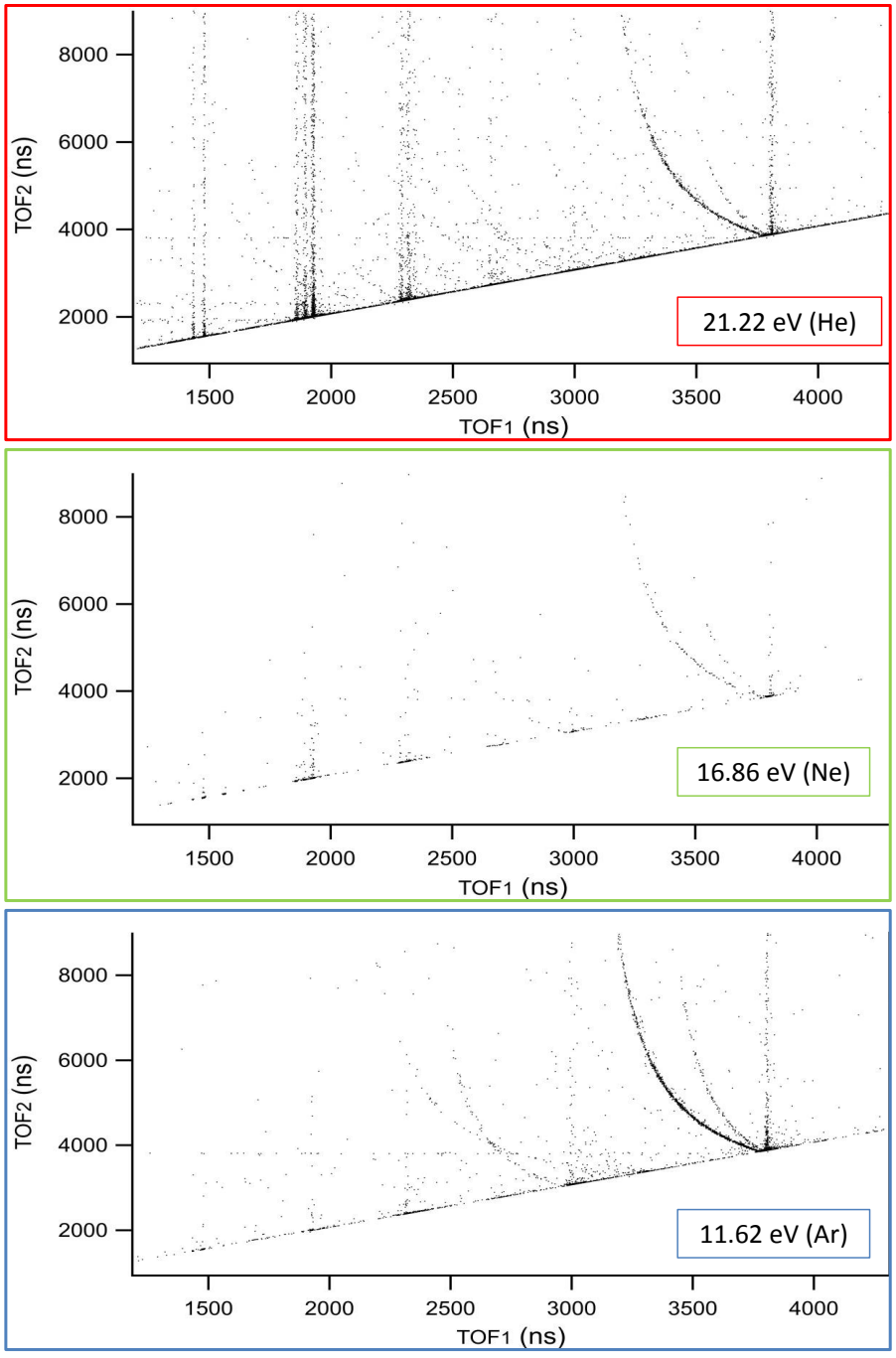


Fig. 1 The cGG ion-neutral coincidence experiments performed at three different photon energies, namely 21.22, 16.85 and 11.62 eV corresponding to main emission lines of the rare gas discharge lamp operated on the CNR-ISM apparatus with He, Ne and Ar gases, respectively.

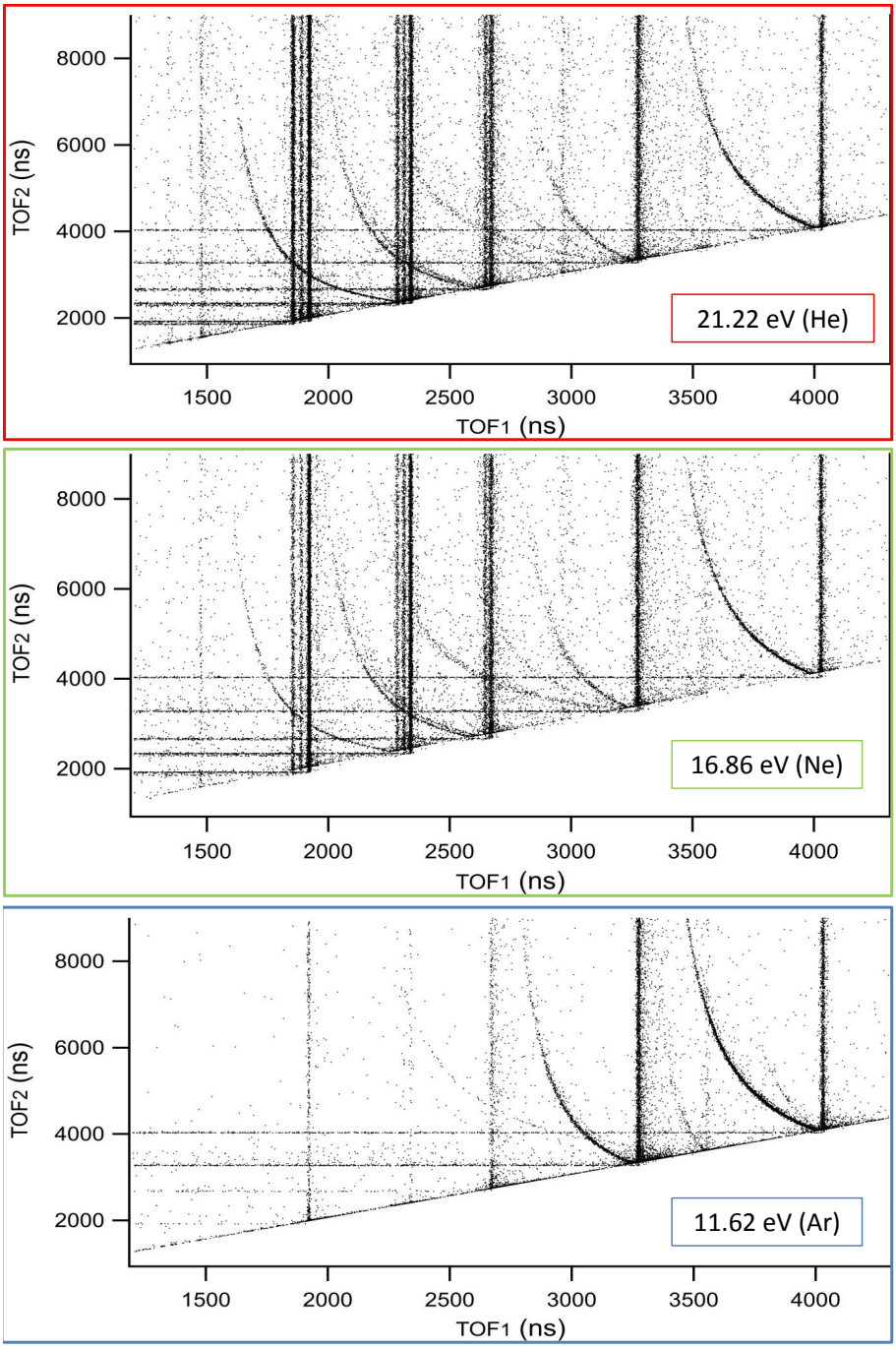


Fig. 2 The cGA ion-neutral coincidence experiments performed at three different photon energies, namely 21.22, 16.85 and 11.62 eV corresponding to main emission lines of the rare gas discharge lamp operated on the CNR-ISM apparatus with He, Ne and Ar gases, respectively.

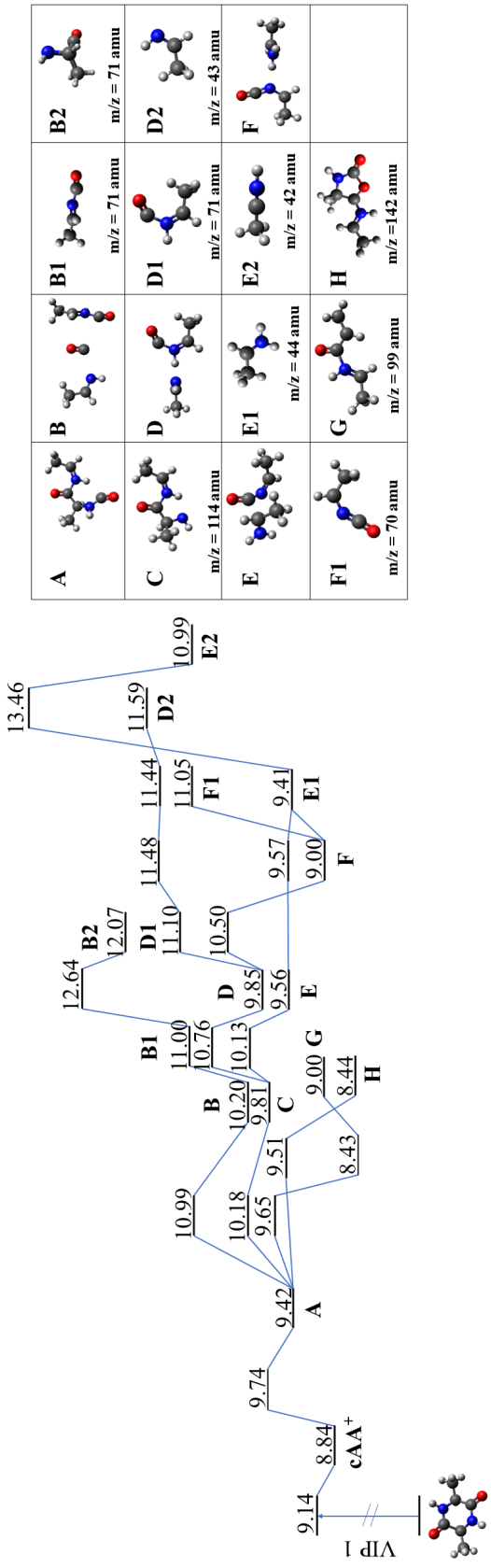


Fig. 3 Stationary points of the potential energy surface corresponding to the fragmentation channels of $cAA^+$. Different minima have been labeled with a letter, from A to H. Relative energies are given in eV at the B3LYP/6-311++G(d,p) level of theory including the zero point energy correction with respect to the most stable isomer of the neutral molecule.

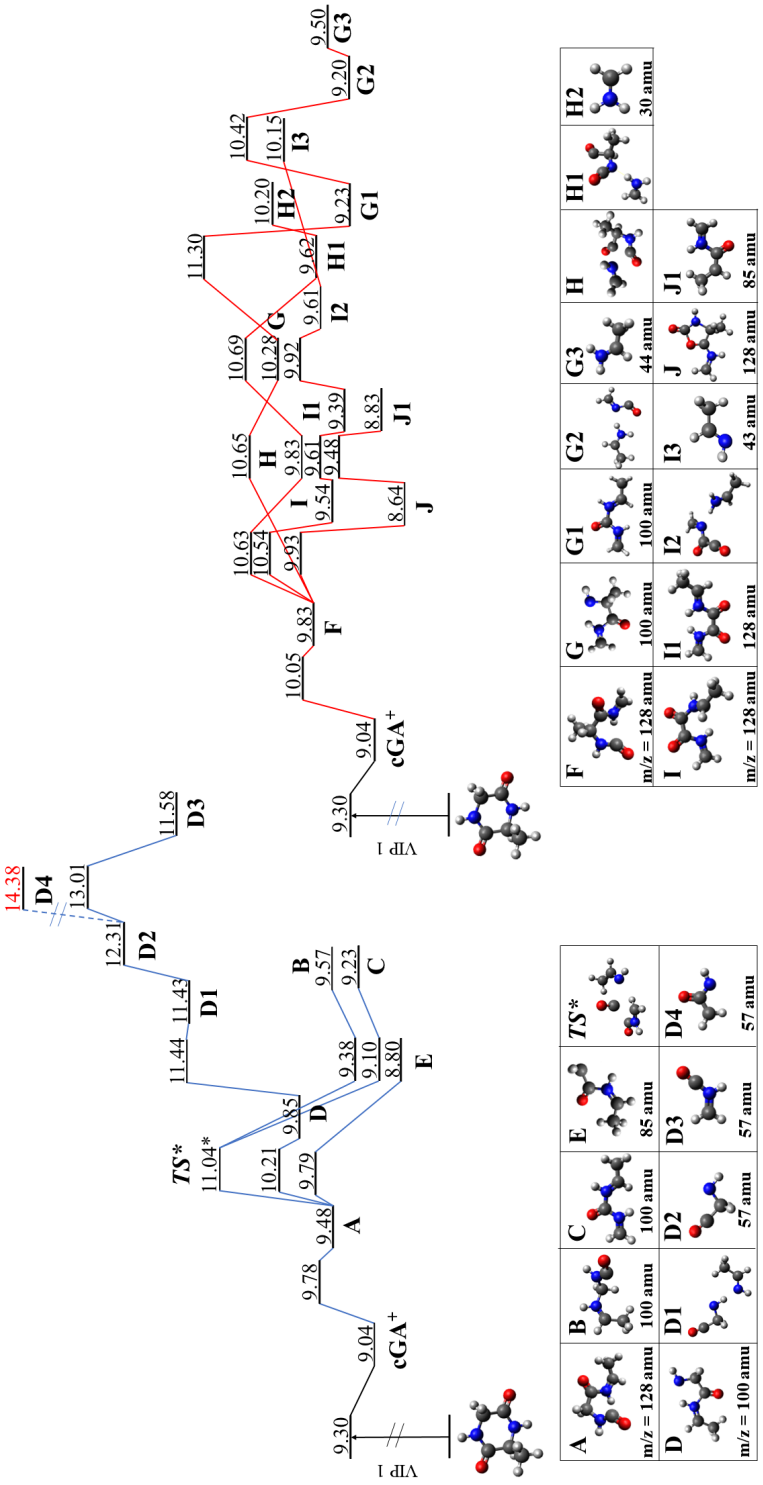


Fig. 4 Stationary points of the potential energy surface corresponding to the fragmentation channels of $cGA^+$. Different minima have been labeled with a letter, from A to J. Relative energies are given in eV at the B3LYP/6-311++G(d,p) level of theory including the zero point energy correction with respect to the most stable isomer of the neutral molecule.

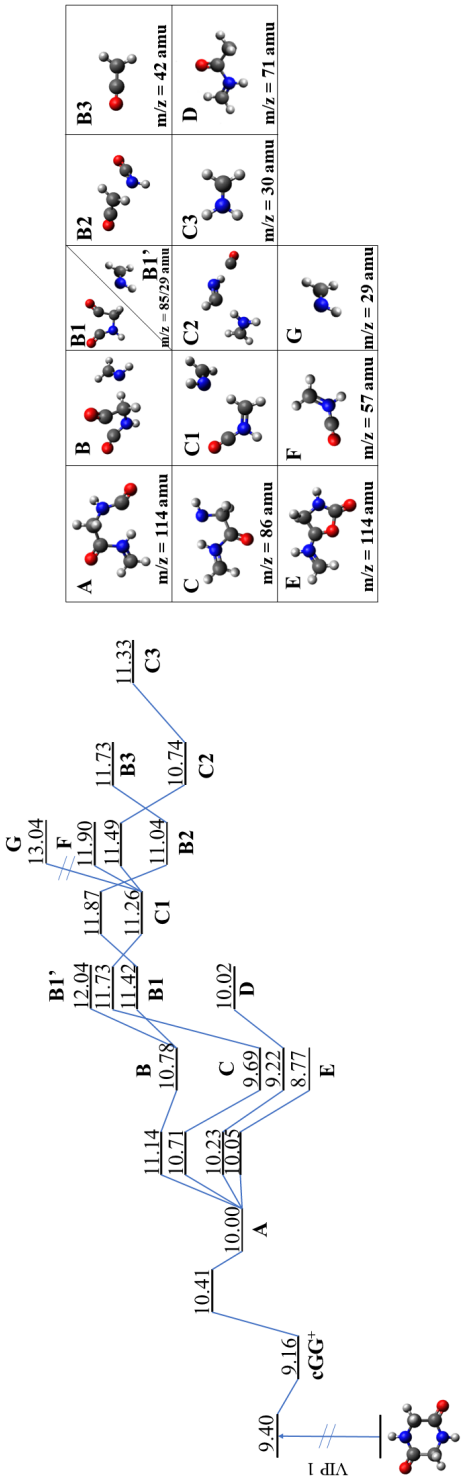


Fig. 5 Stationary points of the potential energy surface corresponding to the fragmentation channels of $cGG^+$. Different minima have been labeled with a letter, from A to F. Relative energies are given in eV at the B3LYP/6-311++G(d,p) level of theory including the zero point energy correction with respect to the most stable isomer of the neutral molecule.

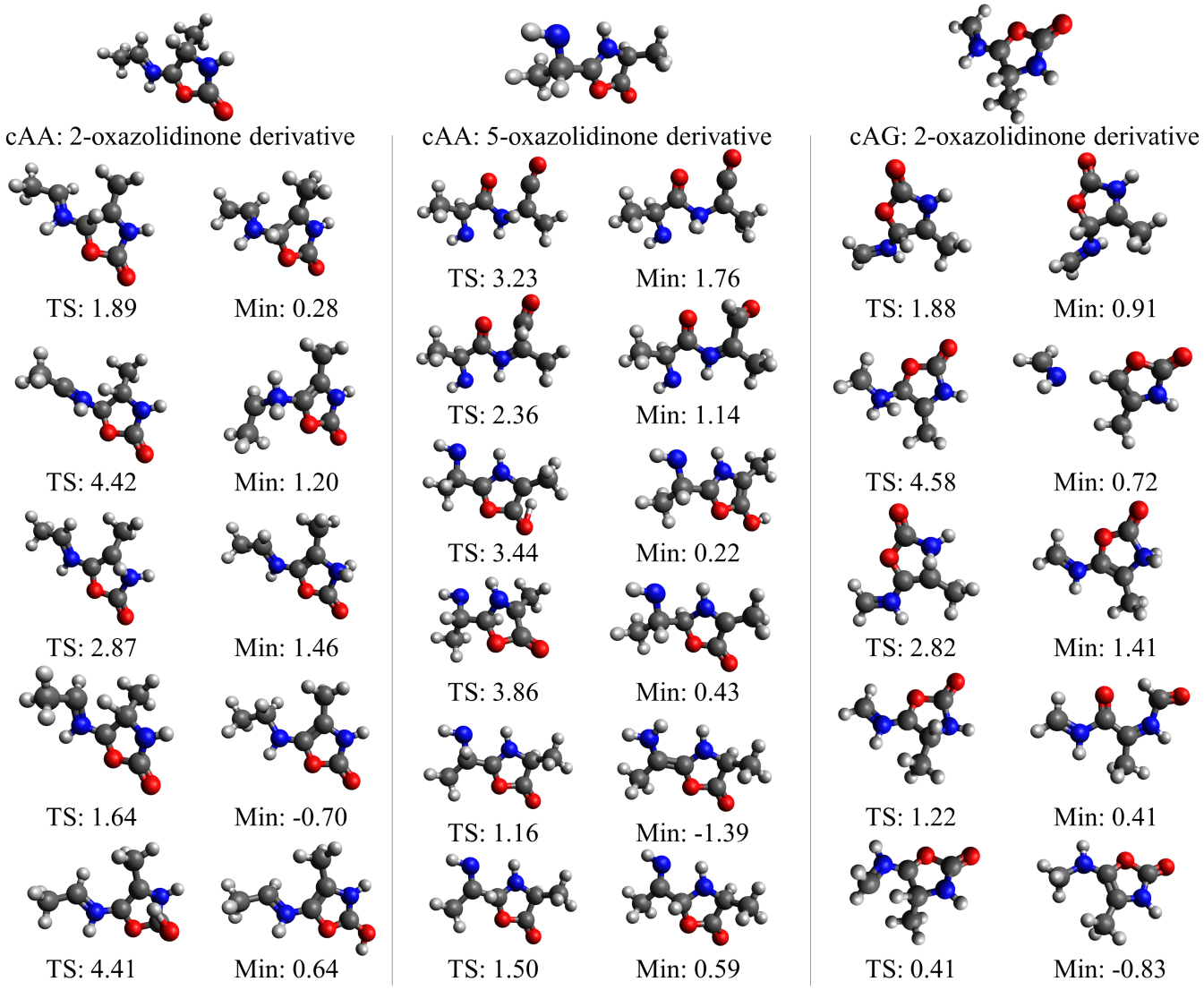


Fig. 6 In this figure are presented all *single-step* mechanisms leading to tautomerization of the three oxazolidinone derivatives already discussed that also lead to the loss of optical purity. All energies are given in eV and referred to each of the oxazolidinone derivatives. Calculations were performed at a M062X/6-311++g(d,p) level of theory.

| $(cAA)^+$ | | | |
|---|---|---|---|
| Channel | m/z | 10 eV | 15 eV |
| $H_{10}C_6N_2O_2^+$ | 142 | 86% | 48% |
| $CH_3CHCONHCHCH_3^+$/**HNCO** | 99 | 5% | 17% |
| $CH_3CHNHCOCHNH^+/CH_3$ | 127 | 5% | 6% |
| $COCH(CH_3)CHNHCO^+/CH_3CHNH$ | 99 | 2% | 0% |
| $CH_3CHCO^+/CH_3CHNH$/**HNCO** | 56 | 1% | 7% |
| $CH_3CHNH/CH_3CHNH^+$/**2CO** | 43 | 1% | 5% |
| $CH_3CHNHCO^+/CH_3CHNH$/**CO** | 71 | 0% | 4% |
| $CH_3CHNHCOCH(CH_3)NH^+$/**CO** | 114 | 0% | 3% |
| $CH_3CHCO/CH_3CHNH^+$/**HNCO** | 43 | 0% | 2% |
| $COCH(CH_3)CHNHCOCH(CH_2)NH/H$ | 141 | 0% | 1% |
| $CH_3CHNHCOH^+/CH_3CHN$/**CO** | 72 | 0% | 1% |
| $CH_3CHCONHCHCH_2^+$/**HNCO**/H | 98 | 0% | 1% |
| $CH_3CHNHCOCHNH^+/CH_3$/**CO** | 99 | 0% | 1% |
| $NH_2CHCH_3^+/CH_3CHNCO$/**CO** | 44 | 0% | 1% |
| $NHCHCO^+/CH_3CHNH/CH_3$/**CO** | 56 | 0% | 1% |
| $CONHCH(CH_3)CO^+/CH_3CHN/H$ | 99 | 0% | 1% |
| $CHNH^+/CH_3CHNH/CH_3$/**2CO** | 28 | 0% | 1% |

Table 1 Statistics of the ADMP molecular dynamics simulations for $cAA^+$: Percentage of all channels for both internal energies. The mass over charge ratio (m/z) of the charged fragments in each channel is also given.

| $(cGA)^+$ | | | |
|---|---|---|---|
| Channel | m/z | 10 eV | 15 eV |
| $H_8C_5N_2O_2^+$ | 128 | 89% | 57% |
| $CH_2NHCOCHCH_3^+$/**HNCO** | 85 | 3% | 7% |
| $CHNHCOCH_2NHCO^+/CH_3$ | 113 | 3% | 2% |
| $CH(CH_3)NHCO^+/NHCH_2$/**CO** | 71 | 2% | 2% |
| $NHCH_2CONHCH^+/CH_3$/**CO** | 85 | 1% | 0% |
| $CH(CH_3)NHCOCH_2NH^+$/**CO** | 100 | 1% | 6% |
| $CH(CH_3)CO^+/NHCH_2$/**HNCO** | 56 | 1% | 6% |
| $CH(CH_3)NH^+/CH_2CO$/**HNCO** | 43 | 0% | 6% |
| $CH(CH_3)NH^+/NHCH_2$/**2CO** | 43 | 0% | 4% |
| $COCHCH_3NHCO^+/NHCH_2$ | 99 | 0% | 2% |
| $CH_2CO^+/CH_3CHNH$/**HNCO** | 42 | 0% | 2% |
| $NHCH_2^+/CH(CH_3)NH$/**2CO** | 29 | 0% | 2% |
| $H_7C_5N_2O_2^+/H$ | 127 | 0% | 1% |
| $CH_2NHCO^+/CH(CH_3)NH$/**CO** | 57 | 0% | 1% |
| $NH_2CH(CH_3)CO^+/NHCH$/**CO** | 72 | 0% | 1% |
| $NHCH_2^+/NCH(CH_3)CO/H$/**CO** | 29 | 0% | 1% |

Table 2 Statistics of the ADMP molecular dynamics simulations for $cGA^+$: Percentage of all channels for both internal energies. The mass over charge ratio (m/z) of the charged fragments in each channel is also given.

| $(cGG)^+$ | | | |
|---|---|---|---|
| Channel | m/z | 10 eV | 15 eV |
| $H_6C_4N_2O_2^+$ | 114 | 63% | 8% |
| $CH_2NHCOCH_2^+$/**HNCO** | 71 | 10% | 5% |
| $NHCH_2^+$/$COCH_2$/**HNCO** | 29 | 5% | 10% |
| $NHCH_2^+$/$NHCH_2$/**2CO** | 29 | 5% | 28% |
| $COCH_2^+$/$NHCH_2$/**HNCO** | 42 | 5% | 17% |
| $NHCH_2CONHCH_2^+$/**CO** | 86 | 5% | 3% |
| $NCH_2CONHCH_2^+$/H/**CO** | 113 | 2% | 2% |
| $NHCH_2CO^+$/$CH_2NH$/**CO** | 57 | 1% | 3% |
| $NH_2CH_2^+$/NHCH/**2CO** | 30 | 1% | 1% |
| $COCH_2NHCO^+$/$NHCH_2$ | 85 | 1% | 0% |
| $NH_2CH_2^+$/COCH/**HNCO** | 30 | 1% | 0% |
| $NHCH^+$/H/$NHCH_2$/**2CO** | 28 | 0% | 5% |
| $CONCH_2^+$/$NHCH_2$/H/**CO** | 56 | 0% | 4% |
| $H_5C_4N_2O_2^+$/H | 113 | 0% | 3% |
| $NH_2CH_2^+$/CONHCH/**CO** | 30 | 0% | 2% |
| $NHCH_2^+$/$NHCH_2CO$/**CO** | 29 | 0% | 2% |
| $CONH_2CH_2^+$/NHCH/**CO** | 58 | 0% | 1% |
| $COCH_2NH_2CO^+$/$NH_2CH_2$ | 84 | 0% | 1% |
| $NHCH_2^+$/$CH_2$/**CO**/**HNCO** | 29 | 0% | 1% |
| $NH_2CH_2^+$/COCH/**HNCO** | 30 | 0% | 1% |
| $NHCH_2^+$/H/$CONCH_2$/**CO** | 29 | 0% | 1% |
| $CH_2COH^+$/HCN/H/**HNCO** | 43 | 0% | 1% |
| $NHCH_2^+$/H/NHCH/**2CO** | 29 | 0% | 1% |

Table 3 Statistics of the ADMP molecular dynamics simulations for $cGG^+$: Percentage of all channels for both internal energies. The mass over charge ratio (m/z) of the charged fragments in each channel is also given.